

Study of PCL mechanism Influence of grid/PAM state on PCL

M. Shiomi^{*}, Y. Okada, Y. Tsuboi, S. Osumi, M. Tsubota

Japan Storage Battery Co. Ltd., Minami-ku, Kyoto, Japan

Abstract

Basic studies to clarify the premature capacity loss (PCL) mechanism have been carried out. It was found that PCL is a phenomenon due to the increase of positive plate resistance, especially the interfacial resistance between the positive grid and the positive active material (PAM) by PbSO_4 formation in the corrosion layer. PCL occurred when the adhesion between the grid and the PAM was poor, H_2SO_4 concentration at the interface between the grid and the PAM is high and the corrosion layer mainly consisted of $\beta\text{-PbO}_2$.

© 2002 Elsevier Science B.V. All rights reserved.

Keywords: Battery; Lead-acid; Positive plate; PCL

1. Introduction

It is well known that the valve-regulated lead-acid (VRLA) battery with an antimony-free positive grid loses discharge capacity earlier than expected under certain conditions, even in a floating application [1]. This phenomenon is called “premature capacity loss (PCL)”.

A number of studies of PCL have been carried out so far. Discharge capacity decreased after a few cycles when the corrosion layer on a pure Pb grid was passivated during cycling, although the discharge capacity did not decline and the corrosion layer was not passivated on a Pb–Sb grid [2]. High current charging was found to delay PCL [3,4]. A barrier layer formed on a Pb–Ca–Sn grid was found to be PbSO_4 when PCL occurred [5,6]. These papers mentioned above dealt with the interface between the grid and the PAM. On the other hand, there were papers dealing with PAM characteristics, especially changes in the connectivity or the size of the positive active material (PAM) particles, which was affected by the charging conditions [7–9].

These papers described how the PCL phenomenon was caused by an increase of positive plate resistance. However, the PCL mechanism is different in every paper.

The objectives of this paper are, first to demonstrate the regions of the positive plate where the PCL phenomenon occurs, and second, to demonstrate the PCL mechanism in a novel apparatus.

2. Location of PCL phenomenon

2.1. Experimental

In order to clarify the sites where the PCL phenomenon proceeds, especially in the PAM and at the grid/PAM interface, the changes in resistance of both the PAM and the grid/PAM interface during were measured cycling of the positive plates by using special positive plates designed by Calabek et al. [10]. Dimensions of this positive plate were $65\text{ mm} \times 75\text{ mm} \times 5\text{ mm}$ and the grid was comprised of six Pb–0.06% Ca–1.5% Sn alloy spines ($\phi 3\text{ mm}$), which were insulated from each other by epoxy resin as illustrated in Fig. 1. In order to cause PCL with in a few cycles, low density PAM of 3.4 g/cm^3 was applied. The experimental cell, an 8 Ah-flooded type, consisted of one positive plate and two negative plates without a separator, was used. 500 ml H_2SO_4 , specific gravity 1.28 (20 °C), was used as electrolyte. This cell was subjected to 2 h discharge at 1 A(0.125CA) to 25%DOD and 5.4 h charge at 0.5 A(0.0625CA) for 20 cycles at 25–30 °C. Discharge capacity and resistances of PAM and grid/PAM interface were measured every 10 cycles.

2.2. Results and discussions

Discharge capacity decreased gradually during 20 cycles as shown in Fig. 2. There was no increase of PAM resistance nor grid/PAM interface resistance in the fully charged state, during 20 cycles. On the other hand, in the discharged state, grid/PAM interface resistances increased more than 10 times

^{*} Corresponding author. Tel.: +81-75-316-3104; fax: +81-75-316-3798.
E-mail address: masaaki_shiomi@gs.nippondenchi.co.jp (M. Shiomi).

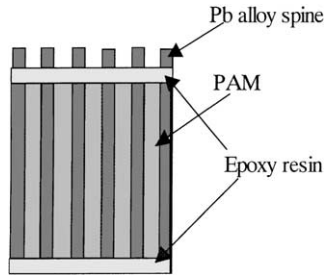


Fig. 1. Positive plate. Pb alloy spines: $\phi 3$ mm, Pb–0.06% Ca–1.5% Sn
PAM: $3.4 \text{ g/cm}^3 \times 75 \text{ g}$.

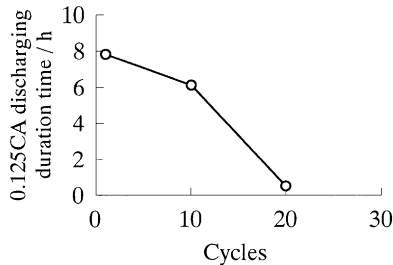


Fig. 2. Change in 0.125C (i.e. 1 A) discharge capacities of an 8 Ah-flooded cell during cycling at 25–30 °C.

from the initial value, although the PAM resistances hardly changed, as shown in Fig. 3. These results obviously showed that PCL is a phenomenon due to an increase of the grid/PAM interface resistance, not due to an increase of the PAM resistance.

The distribution of PbSO_4 across a section of discharged positive plate after 20 cycles was examined by EPMA (Electron Probe Micro Analyzer) as shown in Fig. 4. PbSO_4 was formed at the interfacial area between the grid and the PAM.

From these results, the decrease in the discharge capacity of the positive plate is due to the PCL phenomenon and it was found that PCL is a phenomenon of increasing grid/PAM resistance by PbSO_4 formation in the corrosion layer.

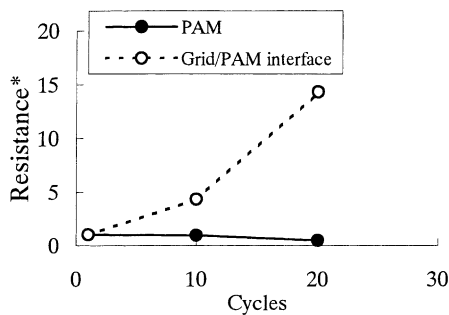


Fig. 3. Changes in PAM resistance and grid/PAM interface resistance at DOD25% during cycling at 25–30 °C. The asterisk (*) indicates ratio to the resistance after first discharge.

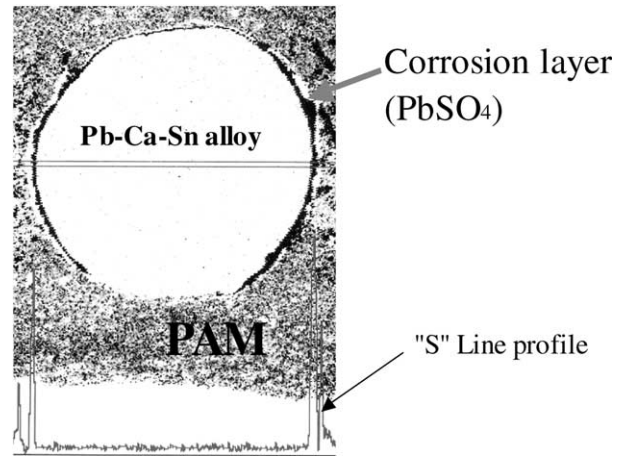


Fig. 4. PbSO_4 distribution in a cross-section of a 25% discharged positive plate after 20 cycles.

3. PCL model

PCL was found to be a phenomenon due to the increase of the interfacial resistance between the grid and the PAM, as described in Section 2. In order to examine the PCL phenomenon in detail, a model representing the positive plate resistance was made, as shown in Fig. 5. In this model, it was assumed that the corrosion layer and the PAM were placed in parallel, because both consist of PbO_2 , and also are physically connected in series. The schematic representation of a positive plate which has failed by PCL is illustrated in Fig. 6.

If the corrosion layer was discharged, R_e^{CL} (resistance of electron transfer from grid to corrosion layer) increased, resulting in a quick drop of discharge voltage. The corrosion layer was preferentially discharged when the corrosion layer resistances ($R_{\text{sol}}^{\text{CL}}, R_r^{\text{CL}}$) become lower or the PAM resistances ($R_{\text{sol}}^{\text{PAM}}, R_r^{\text{PAM}}, R_e^{\text{PAM}}$) become higher.

From this model, the resistance of the discharge reaction of the corrosion layer (R_r^{CL}) and H_2SO_4 resistance around the corrosion layer ($R_{\text{sol}}^{\text{CL}}$) are expected to be the most important factors for the PCL phenomenon, causing an increase of interfacial resistance between the grid and the PAM.

4. Influence of the interface state between the grid and the PAM on PCL performance

To examine the effects of the reactivity (or resistance) of the corrosion layer and the resistance of the H_2SO_4 at the interface between the grid and the PAM, a functional electrode and cell were designed.

4.1. Experimental

A PAM tablet (diameter: $\phi 25$ mm, thickness: 3 mm, density: 3.7 g/cm^3) was prepared as follows. Paste was filled into a small hole, cured under 3BS conditions and formed. After formation, this tablet of PAM was taken off and its surface

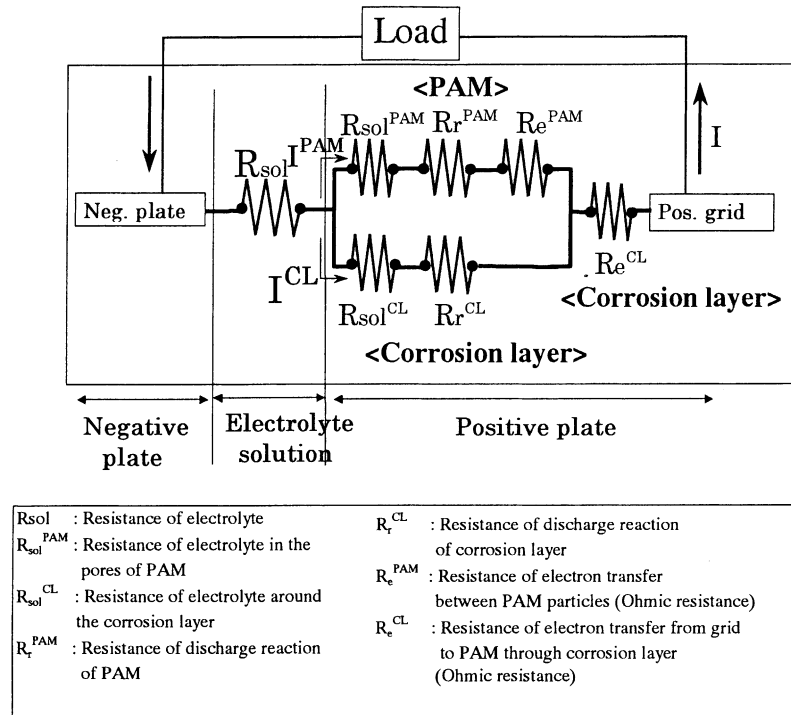


Fig. 5. Resistance model of discharging reaction of positive plate.

was polished to make it smooth. This tablet was put on a flat lead alloy (Pb–0.06% Ca–1.5% Sn) current collector, as shown in Fig. 7, on which corrosion layer was formed in advance. An absorptive glass mat (AGM) separator, a conventional negative plate and a weight were put on the PAM tablet. A total of 1.30 specific gravity H₂SO₄ was retained in the PAM, AGM and negative active material (NAM) before loading. Fig. 8 shows the construction of the “Tablet plate” cell.

The resistance of the electrolyte, especially at the interface area between the current collector (Pb alloy) and the PAM, can be changed by regulating the weight and also by adding a different concentration of electrolyte directly on the corrosion layer.

A light weight means a relatively small adhesion between the current collector (corrosion layer) and the PAM. This

would cause high mobility and low resistance of H₂SO₄ around the corrosion layer area. Thus, the effect of electrolyte resistance at the interface area between the current collector and the PAM can be examined with this tablet plate cell.

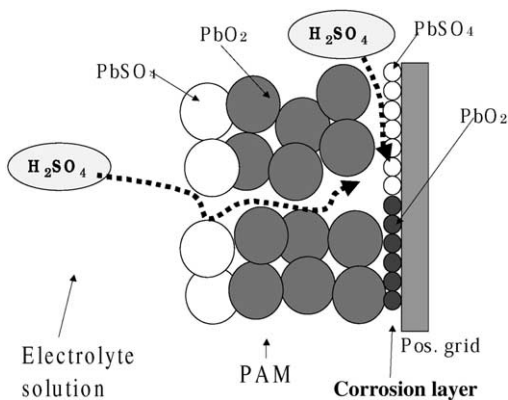


Fig. 6. Schematic representation of a positive plate which was failed by PCL phenomenon.

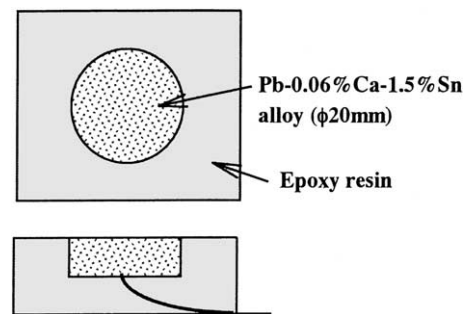


Fig. 7. Current collector.

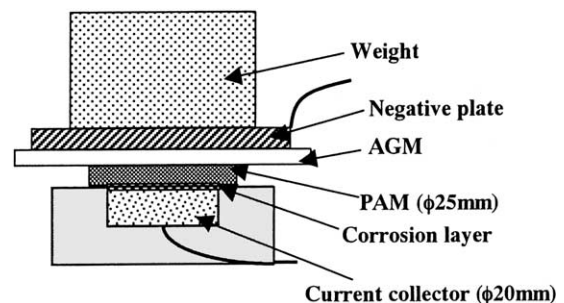


Fig. 8. “Tablet plate” cell.

Table 1
Details of the cells

Cell no.	Corrosion layer	Specific gravity of H ₂ SO ₄ in AGM separator, PAM and NAM	Specific gravity of H ₂ SO ₄ around corrosion layer	Weight (g)
1	β-PbO ₂ rich ^a	1.30	1.30	300
2	β-PbO ₂ rich	1.30	1.30	450
3	β-PbO ₂ rich	1.30	1.30	600
4	β-PbO ₂ rich	1.30	1.30	1000
5	β-PbO ₂ rich	1.30	1.30	2000
6	β-PbO ₂ rich	1.30	1.40	2000
7	α-PbO ₂ rich ^b	1.30	1.40	2000

^a One discharge–charge cycle after anodic oxidation (100 mA × 48 h in specific gravity 1.05 of H₂SO₄).

^b Anodic oxidation: 100 mA × 48 h in 0.1N NaOH.

Two kinds of compounds (α, β-PbO₂) were formed in the corrosion layer by anodic oxidation of the Pb alloy current collector before the PAM tablet was put on, in order to examine the effect of the corrosion layer reactivity on the PCL phenomenon. In general, it is known that β-PbO₂ is more reactive than α-PbO₂ and shows a higher utilization rate when discharged.

The α-PbO₂ corrosion layer was made by anodic oxidation in 0.1 N-NaOH. β-PbO₂ was made by anodic oxidation and one discharge–charge cycle in specific gravity 1.05 of H₂SO₄. The composition of the cycle corrosion layer cannot be changed without changing other material conditions, such as PAM composition and physical characteristics, if conventional positive plates are used. However, with this tablet plate the composition of the corrosion layer can be changed without changing any other material conditions.

Details of the cell construction are described in Table 1. These cells were subjected to 150 mA (i.e. 27.5 mA per gram of PAM) discharge at 25–30 °C and discharge voltages were measured.

4.2. Results and discussions

The changes of discharge voltage are shown in Figs. 9 and 10. The cell voltage dropped abruptly at short time discharge on the cells with weights of less than 450 g (14 kPa). There

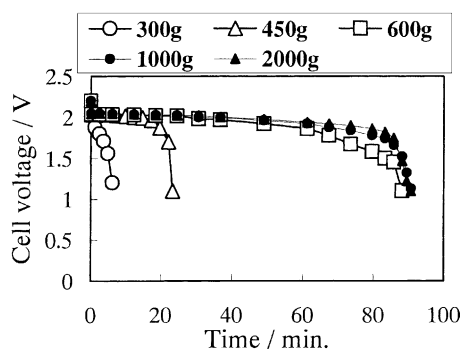


Fig. 9. Effect of the weight on 150 mA discharging characteristics at 25–30 °C.

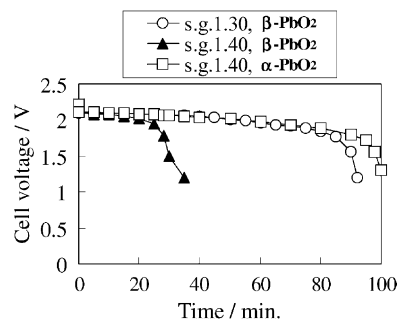


Fig. 10. Effect of the specific gravity of H₂SO₄ at the interface of corrosion layer and PAM and composition of corrosion layer on 150 mA discharging characteristics at 25–30 °C.

were no effects on the cells with the weight of more than 600 g (19 kPa). The discharge voltage decline of the former is not due to just the poor contact between the current collector and the PAM, because the discharge voltages of all the cells at the beginning of discharge are all the same, notwithstanding the weight difference. Therefore, this decline in discharge capacity with the light weight cells is expected to be due to the PCL phenomenon.

It was found from these results that PCL was largely affected by the adhesion between the current collector (β-PbO₂ corrosion layer) and the PAM, and the increase of internal resistance or discharging of the corrosion layer was caused during discharge.

The discharge voltage of the positive electrode with specific gravity 1.40 of H₂SO₄ on the β-PbO₂ corrosion layer (Cell no. 6) dropped after a shorter time than that with the specific gravity 1.30 of H₂SO₄ (Cell no. 5), although the discharge voltages at the beginning of the discharge of both of the cells were not different. In this experiment, a 2000 g weight was applied and it could not have failed by poor adhesion. It was found that high H₂SO₄ concentration around the β-PbO₂ corrosion layer accelerated PCL, even if the adhesion between the current collector and the PAM was good. It might be because the electrode potential of the corrosion layer became higher and the corrosion layer was preferentially discharged when the H₂SO₄ concentration around the corrosion layer increased.

On the other hand, the positive electrode with specific gravity 1.40 of H₂SO₄ on the α-PbO₂ corrosion layer (Cell no. 7) did not show PCL behavior at all. These experimental results proved that the effect of corrosion layer composition on the PCL phenomenon was much larger than that of the local H₂SO₄ concentration. Especially the α-PbO₂ corrosion layer could prevent PCL, even in a high H₂SO₄ concentration around corrosion layer. This may be because of the reactivity of the electrode potential difference between α-PbO₂ and β-PbO₂.

5. Changes of interfacial states between the grid and the PAM during cycling

The changes of H₂SO₄ concentration at the interface between the current collector and the PAM and changes

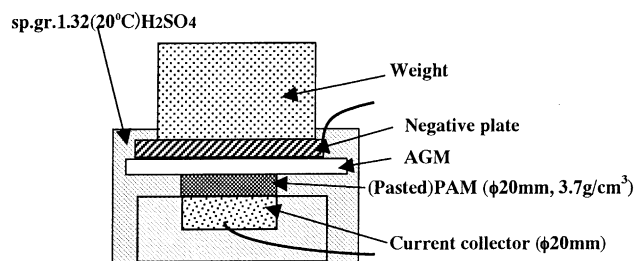


Fig. 11. Experimental cell.

in the composition of the corrosion layer with the number of cycles were examined.

5.1. Experimental

We manufactured electrodes with PAM (diameter: $\phi 20$ mm, thickness: 3 mm, density: 3.7 g/cm^3) on a Pb–0.06% Ca–1.5% Sn alloy current collector, as shown in Fig. 11. The PAM was pasted on a Pb alloy current collector directly and cured in 3BS conditions. Then, an AGM separator, a negative plate of larger capacity than the positive plate and a weight (1000 g) were put on it, and 1.32 specific gravity H_2SO_4 was poured into the cell. Thus, 300 mAh capacity cells were constructed. The cells were subjected to the cycling test of 100 mA discharge for 20 min and 15 mA charge for 200 min at 50°C . The specific gravity of the H_2SO_4 around the grid/PAM interface and the chemical composition of the corrosion layer during cycling were periodically measured. Cells with a Pb–3% Sb–0.25% As alloy current collector were also tested, and the cells with Pb–0.06% Ca–1.5% Sn alloy current collector were subjected to another cycling test with high current (300 mA) charging.

In order to measure the H_2SO_4 concentration at current collector/PAM interface, a thermogravimetry (TG) method was applied. A small portion of PAM or corrosion layer with H_2SO_4 and H_2O was taken and the changes of their weight were observed with increasing temperature. The H_2SO_4 concentration could be calculated by measuring the weight of H_2O and H_2SO_4 respectively. The chemical compositions of the corrosion layers were analyzed by the X-ray diffraction method. The diffraction line, characteristic for $\alpha\text{-PbO}_2$ was that of 3.12 \AA interplanar distance and those for $\beta\text{-PbO}_2$ are 2.80 and 3.50 \AA . Intensity of $\beta\text{-PbO}_2$ peak was calculated as $1/2(I_{p_{2.80\text{ \AA}}} + I_{p_{3.50\text{ \AA}}})$.

5.2. Results and discussion

The changes of the cell voltage at the end of the discharge during cycling are shown in Fig. 12. The discharge voltage quickly decreased after only 35 cycles for the cell of Pb–0.06% Ca–1.5% Sn alloy current collector with 15 mA charging, although it did not decrease for the cells of both the Pb–0.06% Ca–1.5% Sn alloy current collector with

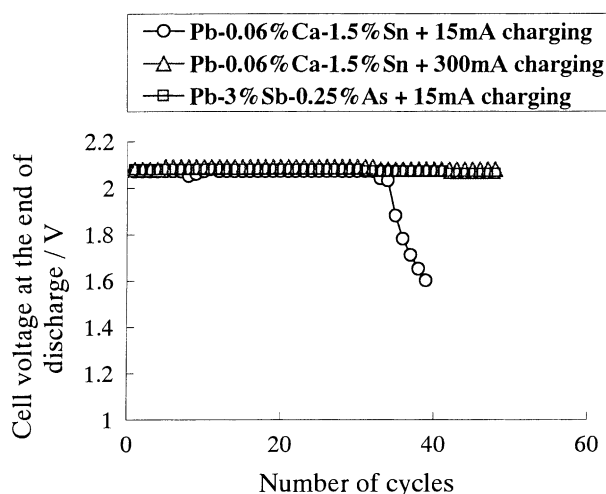


Fig. 12. Changes in the end-of-discharge voltage of 300 mAh cells.

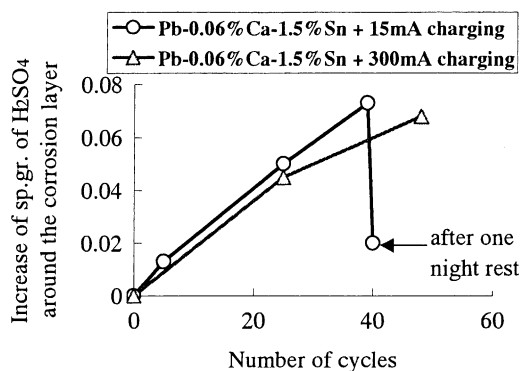
300 mA charging and the Pb–3% Sb–0.25% As alloy current collector with 15 mA charging.

Some of the cells were disassembled, and the specific gravity of the H_2SO_4 around the current collector/PAM interface and the X-ray diffraction pattern of the corrosion layer were measured.

The changes of the specific gravity of the H_2SO_4 around the current collector (Pb–0.06% Ca–1.5% Sn alloy)/PAM interface are shown in Fig. 13.

Surprisingly, the specific gravity of the H_2SO_4 around current collector (Pb–0.06% Ca–1.5% Sn alloy)/PAM interface increased with the number of the cycles, under both 15 mA charging and 300 mA charging. They decreased and returned to a lower value after one night left standing. The above results would hardly give a mechanism involving an increasing of H_2SO_4 concentration around current collector, however, the H_2SO_4 concentration certainly affects PCL, as already described.

The changes of $\alpha\text{-PbO}_2$ peak intensity ratio to $(\alpha + \beta)\text{-PbO}_2$ peak intensity of the X-ray diffraction pattern are depicted in Fig. 14. The $\alpha\text{-PbO}_2$ peak intensity significantly

Fig. 13. Changes in specific gravity of H_2SO_4 around the current collector (Pb–0.06% Ca–1.5% Sn alloy)/PAM interface.

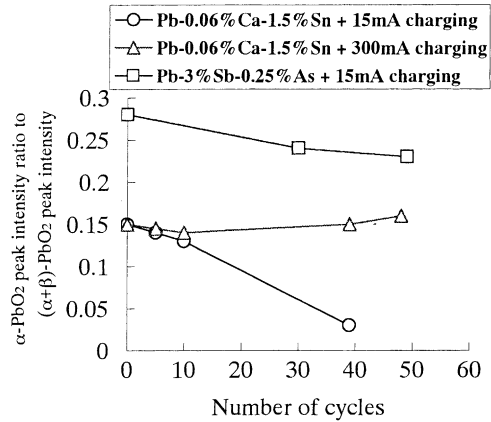


Fig. 14. Changes in α -PbO₂ peak intensity ratio to $(\alpha + \beta)$ -PbO₂ peak intensity of X-ray diffraction pattern.

decreased only for the Pb–0.06% Ca–1.5% Sn alloy electrode cycled with 15 mA charging during cycling.

On the other hand, the α -PbO₂ peak intensities for Pb–0.06% Ca–1.5% Sn alloy electrode cycled with 300mA charging and also for Pb–3% Sb–0.25% As alloy electrode, held constant during cycling.

It is well known that high rate charging and a Pb–Sb alloy positive grid can suppress the PCL phenomenon. This might be due to the fact that the amount of α -PbO₂ in the corrosion layer on a Pb alloy grid did not decrease with the number of cycles.

From these results, it was found that PCL occurred when adhesion between the current collector and the PAM was poor and the H₂SO₄ concentration around the corrosion layer was high and that PCL did not occur when the corrosion layer is mainly consisted of α -PbO₂.

The positive plate resistance model was proposed. It showed that PCL was not a strange or a special phenomenon, but it was found that the reactivity of the corrosion layer and the resistance of the H₂SO₄ around the corrosion layer would affect PCL.

6. Conclusions

1. PCL was a phenomenon due to the increase of the positive plate resistance, especially at the interface between the grid and the PAM.
2. A simple PCL model was proposed. This model gave the important factors on PCL, such as the reactivity of the corrosion layer and the resistance of H₂SO₄ at the interface between the grid and the PAM.
3. PCL occurred when the adhesion between the grid and the PAM was poor, the H₂SO₄ concentration at the interface between the grid and the PAM is high and the corrosion layer mainly consisted of β -PbO₂.
4. The H₂SO₄ concentration at the interface between grid the and the PAM increased with the number of cycles operated under certain conditions and the positive plate with a Pb–Sb grid with conventional charging or a Pb–Ca grid operated under high rate charging conditions had higher amounts of α -PbO₂, which was stable during charge and discharge cycling.

References

- [1] G. Karlsson, in: Proceedings of the 21st International Telecommunication Energy Conference, Copenhagen, Denmark, 6–9 June 1999, pp. 21–23.
- [2] M.K. Dimitrov, D. Pavlov, J. Power Sources 46 (1993) 203.
- [3] D. Pavlov, G. Petkova, M. Dimitrov, M. Shiomi, M. Tsubota, J. Power Sources 87 (2000) 39.
- [4] Y. Okada, K. Takahashi, M. Tsubota, in: Proceedings of the 11th International Electric Vehicle Symposium, Florence, Italy, 27–30 September 1992, 6.01.
- [5] M. Kosai, S. Yasukawa, S. Osumi, M. Tsubota, J. Power Sources 67 (1997) 43.
- [6] M. Tsubota, S. Osumi, M. Kosai, J. Power Sources 33 (1991) 105.
- [7] A. Winsel, E. Voss, U. Hullmeine, J. Power Sources 30 (1990) 209.
- [8] W. Borger, U. Hullmeine, H. Laig-Horstebroek, E. Meissner, in: T. Keily, B.W. Baxter (Eds.), Power Sources, vol. 12, 1989, p. 131.
- [9] E. Meissner, J. Power Sources 46 (1993) 231.
- [10] M. Calabek, K. Micka et al., J. Power Sources 62 (1996) 161.